Published online 25 February 2010 *Nucleic Acids Research, 2010, Vol. 38, No. 11* ***3655–3671***
doi:10.1093/nar/gkq098

hMSH5 is a nucleocytoplasmic shuttling protein whose stability depends on its subcellular localization

François Lahaye[1], Françoise Lespinasse[1], Pascal Staccini[2], Lucile Palin[1], Véronique Paquis-Flucklinger[1] and Sabine Santucci-Darmanin[1,*]

[1]FRE 3086 'Instabilité génétique: Maladies rares et cancers', Université de Nice Sophia-Antipolis, CNRS and [2]Stic, Université de Nice-Sophia Antipolis, Faculté de Médecine, Avenue de Valombrose 06107, Nice Cedex 2, France

Received April 24, 2009; Revised February 2, 2010; Accepted February 3, 2010

ABSTRACT

MSH5 is a MutS-homologous protein required for meiotic DNA recombination. In addition, recent studies suggest that the human MSH5 protein (hMSH5) participates to mitotic recombination and to the cellular response to DNA damage and thus raise the possibility that a tight control of hMSH5 function(s) may be important for genomic stability. With the aim to characterize mechanisms potentially involved in the regulation of hMSH5 activity, we investigated its intracellular trafficking properties. We demonstrate that hMSH5 possesses a CRM1-dependent nuclear export signal (NES) and a nuclear localization signal that participates to its nuclear targeting. Localization analysis of various mutated forms of hMSH5 by confocal microscopy indicates that hMSH5 shuttles between the nucleus and the cytoplasm. We also provide evidence suggesting that hMSH5 stability depends on its subcellular compartmentalization, hMSH5 being much less stable in the nucleus than in the cytoplasm. Together, these data suggest that hMSH5 activity may be regulated by nucleocytoplasmic shuttling and nuclear proteasomal degradation, both of these mechanisms contributing to the control of nuclear hMSH5 content. Moreover, data herein also support that in tissues where both hMSH5 and hMSH4 proteins are expressed, hMSH5 might be retained in the nucleus through masking of its NES by binding of hMSH4.

INTRODUCTION

Despite being a member of the DNA mismatch repair (MMR) family of proteins, the MutS homolog MSH5 does not appear to participate in mismatch repair in mammalian cells. Instead, this protein, together with a second MutS-like protein called 'MSH4', is essential for meiosis. Several lines of evidence strongly suggest that the MSH4-MSH5 heterodimer is essential for the processing and/or the stabilization of meiotic DNA recombination intermediates (1–3). Nevertheless, recent findings also support the view that human MSH4 and MSH5 proteins might be involved in processes other than meiotic recombination and might even function independently of one another (4).

These proposals are notably based on expression data which showed that *MSH4* and *MSH5* transcripts are present in human non-meiotic tissues (4), and that *hMSH4* exhibits a limited expression profile whereas *hMSH5* mRNA are detected in a broad spectrum of tissues (5–10). Protein–protein interaction data and functional studies also strengthen the assumption that hMSH4 and hMSH5 proteins are involved in various cellular processes through their interactions with different partners. hMSH4 interacts with VBP1 (9), which is suspected of being involved in microtubule assembly (11) and which competes with hMSH5 for binding to hMSH4 (9). Conversely, hMSH5 has been shown to interact with c-Abl (12), a tyrosine kinase implicated in the regulation of DNA recombination and DNA damage signaling. This interaction facilitates the activation of c-Abl tyrosine kinase and induces the tyrosine phosphorylation of hMSH5 in response to ionizing radiation, which in turn favors the dissociation of the hMSH4-hMSH5

*To whom correspondence should be addressed. Tel: +33 4 93 37 70 56; Fax: +33 4 93 37 70 33; Email: santucci@hermes.unice.fr

The authors wish it to be known that, in their opinion, the first two authors should be regarded as joint First Authors.

heterocomplex (12). The hMSH5–c-Abl interaction promotes ionizing radiation-induced apoptosis (13). RNAi-mediated hMSH5 silencing reduces apoptosis in irradiated cells and conversely, the overexpression of hMSH5 alone is sufficient to increase the radiation-induced apoptotic response (13), which implies that hMSH4 is not implicated in this process. hMSH5 has also been found to interact with HJURP and MRE11 in a human cell line derived from a lung adenocarcinoma (14). HJURP is a Holliday junction binding protein (14), and MRE11 is a crucial enzyme for DNA double-strand break repair (15). Taken together, these findings strongly suggest that hMSH5 is involved in DNA damage signaling and mitotic DNA recombination and, thereby, in the maintenance of genomic stability. Furthermore, the dimerization of hMSH5 and hMSH4 would appear not to be required for all hMSH5 functions. These observations, in addition to the fact that the *hMSH5* locus (6p21.33) has been identified as a new locus for susceptibility to lung cancer (16), has emphasized the necessity for further investigating the function(s) exerted by the hMSH5 protein and the mechanisms involved in the regulation of its various, as-yet undefined activities.

Shuttling between the nucleus and the cytoplasm has emerged in the last few years as an important regulatory mechanism for multifunctional proteins involved in DNA repair pathways and maintenance of genetic stability, such as BRCA1, BRCA2, p53 and FANCA (17–19). Interestingly, a previous study has led to the proposal that nucleocytoplasmic trafficking may constitute a regulatory mechanism for MSH4 functions (20). As a first step toward analyzing the mechanisms involved in the control of hMSH5 functions, we investigated the cellular trafficking properties of hMSH5. Trafficking of most proteins larger than 60 kDa through nuclear pore complexes is an active process mediated by nuclear import and export receptors, which bind to nuclear localization signals (NLS) or nuclear export signals (NESs) within cargo proteins (21). Classical NLS sequences contain one or two clusters of positively charged amino acids (22). The most common NES are characterized by short hydrophobic leucine-rich regions that are generally recognized by the export receptor CRM1 (23).

Here, we provide the first evidence that hMSH5 is a nucleocytoplasmic shuttling protein that actively enters and exits the nucleus. We demonstrate that hMSH5 contains a conserved classical monopartite NLS and a conserved C-terminal NES motif that mediate nuclear export through the CRM1-dependent pathway. In addition, our data indicate that the stability of hMSH5 is related to its subcellular localization. Our experiments suggest that the half-life of hMSH5 is markedly reduced in the nucleus and that this is dependent on the proteasome. Therefore, our results raise the possibility that hMSH5 nuclear activity may be regulated by both nucleocytoplasmic shuttling and proteasomal degradation. Finally, we provide new insights into the reciprocal regulation of the subcellular localizations of hMSH5 and hMSH4 through their dimerization.

MATERIAL AND METHODS

Cell culture and transfections

HeLa cervical carcinoma cells were from the American Type Culture Collection and maintained in Eagle's Minimum Essential Medium (EMEM) supplemented with 10% fetal calf serum and antibiotics. Cells seeded onto 60-mm sterile dishes or glass coverslips in culture dishes were transfected by using either a standard calcium phosphate method or FuGene HD reagent according to the manufacturer's instructions (Roche Applied Science). Twenty-four hours after transfection, Leptomycin B (LMB, Biomol) was added for 6 h (except when indicated) at a final concentration of 18.5 nM to inhibit CRM1-dependent nuclear export. The proteasome inhibitor MG132 (Biomol) and the protein synthesis inhibitor cycloheximide (Sigma–Aldrich) were added to transfected cells for the indicated periods of time at concentration of 10 μM and 50 μg/ml, respectively. The actinomycin D (Sigma-Aldrich) was used at a final concentration of 5 μg/ml.

Antibodies

Mouse monoclonal anti-GFP (B-2) and goat polyclonal anti-Lamin B (C-20) were from Santa Cruz Biotechnology; mouse monoclonal anti-Flag (M2) and mouse monoclonal anti-ß-tubulin were purchased from Sigma–Aldrich, mouse monoclonal anti-Hsp90α and mouse monoclonal anti-Poly(ADP-Ribose) Polymerase-1 (PARP-1) were from Calbiochem. Secondary antibodies used in western blotting experiments were either goat anti-mouse immunoglobulin (IgG) or rabbit anti-goat IgG, conjugated with horseradish peroxydase (Dako).

Plasmid constructions and mutagenesis

pEGFP-C1-hMSH5 and the plasmid encoding DsRed-hMSH4 have been described previously (20). To generate the GFP-N1-hMSH5 protein construct, the hMSH5 cDNA was amplified by polymerase chain reaction (PCR) with primers containing terminal restriction sites. The resulting products were digested and ligated in frame into the XhoI–BamHI sites of pEGFP-N1 (Clontech). For the expression of hMSH5 deletion mutants as GFP fusion proteins, specific regions of the hMSH5 cDNA were PCR-amplified, digested and cloned between XhoI and BamHI sites of pEGFP-C1 (Clontech). The pFLAG-hMSH5 plasmid was generated by insertion of the hMSH5 coding sequence, which was amplified by PCR, into BamHI/PstI sites of the pCMV-3Tag-1 A vector (Stratagene).

The plasmids pRev(1.4)-GFP and pRev(1.4)-NES-GFP were kind gifts from Dr. Beric Henderson (Westmead Institute for Cancer Research, Australia) and have been described elsewhere (24). Oligonucleotides (5′-GATCCAC AGACA**TTAGTGGATAAGTTTATGAAACTGGATTT GG**AAGATCCTAACCTGGACTTA-3′ and 5′-CCGGT AAGTCCAGGTTAGGATCTTC**CAAATCCAGTTTCA TAAACTTATCCACTAA**TGTCTGTG-3′) were annealed to produce a double-stranded DNA fragment flanked by BamH1 and AgeI termini and that encodes the putative

wild-type hMSH5 NES (bold characters). This DNA fragment was inserted between the Rev(1.4) and the GFP coding sequences of pRev(1.4)-GFP to produce pRev(1.4)-hMSH5-NES-GFP. The vector pRev(1.4)-hMSH5-NES^{mut}-GFP containing the hMSH5 NES bearing mutations in the four consensus residues (L802A, F806A, L809A and L811A) was constructed by using the same strategy and the following oligonucleotides 5′-GATCCACAGACA**GCAGTGGATA AGGCTATGAAAGCGGATGCG**GAAGATCCTAACC TGGACTTA-3′ and 5′-CCGGTAAGTCCAGGTTAGG ATCTTC**CGCATCCGCTTTCATAGCCTTATCCAC TGC**TGTCTGTG-3′.

The pHM830 plasmid encodes the GFP-β-galactosidase fusion protein (called GFP-βgal in the following text). The pHM840 vector allows the expression of the GFP-(SV40-LT)NLS-β-galactosidase protein, referred to as GFP-(SV40-LT)NLS-βgal. Both pHM830 and pHM840 were kindly provided by Dr Thomas Stamminger (Institute for Clinical and Molecular Virology, University Hospital Erlangen, Germany) and have been described previously (25). hMSH5 cDNA fragments corresponding to residues 1–405, 410–549, 508–558, 550–750 and 700–834 of the protein were obtained by PCR using primers incorporating a NheI site at the 5′-end and a SacII site at the 3′-end. The resulting fragments were inserted into the NheI/SacII-digested pHM830 plasmid. The construct containing the putative NLS motif of the hMSH5 protein was generated by annealing two oligonucleotides (5′-CGC GGGGCCAGGATGAG**AAAAAGCGAAGA**CTGGTG GGCTGTAGAG-3′ and 5′-CTCTACAGCCCACCAG**T CTTCGCTTTTT**CTCATCCTGGCCCCGG-3′) and inserting the resulting double-stranded DNA fragment in frame into the NheI–SacII sites of pHM830. The putative hMSH5 NLS sequence is indicated by boldface letters.

The various full-length GFP-hMSH5-NES and GFP-hMSH5-NLS punctual mutants were generated using the QuikChange-XL Site-Directed Mutagenesis kit (Stratagene). Oligonucleotide sequences used for PCR amplification and for site-directed mutagenesis are available upon request. All constructs described above were verified by DNA sequencing.

Fluorescence microscopy and quantitation of subcellular distribution

Cells transiently transfected with GFP and/or Ds-Red fusion constructs, were grown on glass coverslips and treated or not with leptomycin B as described above. Thereafter, cells were fixed in 0.2 M phosphate buffer (pH 7.4) with 4% paraformaldehyde and mounted on slides with Mowiol 4-88 reagent (Calbiochem) containing DAPI (4′,6-diamidino-2-phenylindole, Sigma–Aldrich) in order to stain nuclei. Cells were visualized with a Zeiss LSM 510 META confocal laser scanning microscope by using a 63× oil-immersion objective, appropriate filter sets, argon (488 nm) and helium-neon (543 nm) and a blue diode (405 nm) lasers. Images of fluorescent cells were captured within the linear range of the digital camera (CCD camera, model C 4880; Hamamatsu Phototonics).

For full-length, truncated or point-mutated hMSH5 fusion proteins (Figures 1–3, 6 and 8) and for DsRed-hMSH4 (Figure 8), quantitative analyses were performed according to previously described procedures (26–29), with slight modifications. Briefly, for each cell analyzed, AxioVision Release 4.5 software (Zeiss) was used to quantify GFP or DsRed fluorescence intensities from a confocal z-section that cuts through the middle of the nucleus: the mean fluorescence in the entire cell area (nuclear plus cytoplasmic or N + C) and the mean fluorescence in the nucleus area (N), as delineated by DAPI staining, were determined after subtraction of the background signal. For each cell, these measurements were used to calculate the percent fluorescence value for the nuclear compartment (N/N + C ratio). As many as 30–35 cells were analyzed for each construct and each condition (incubation of transfected cells in the absence or presence of leptomycin B). This was repeated three times and the mean value of the N/N + C ratio with standard deviation was calculated for each protein and each condition from these three independent experiments. Comparison of mean values used a *t*-test procedure and was performed with Minitab 13 software, a value of 0.05 was chosen as the level of significance.

To evaluate the activity of the hMSH5 nuclear export sequence when this motif was fused to an heterologous protein (Figure 4), quantitative analyses were performed as described in (24). Briefly, the subcellular distribution of each pRev(1.4)-GFP-derived construct was analyzed by evaluating the percentage of cells with either exclusively nuclear (N), nuclear and cytoplasmic (NC) or exclusively cytoplasmic (C) GFP fluorescence. At least 200 cells were scored for each transfection assay. The mean and standard deviation values from three independent transfection experiments were then calculated for each pRev(1.4)-GFP-derived construct. The same procedure was used to quantify the subcellular distribution of the various pHM830-derived constructs used to characterize potential nuclear localization signals within hMSH5 (Figure 5).

In vivo export pRev1.4 assay

HeLa cells were transfected with either pRev(1.4)-GFP, pRev(1.4)-NES-GFP or pRev(1.4)-MSH5-NES-GFP. At 24 h after transfection, cells were treated with either cycloheximide and actinomycin D or cycloheximide and LMB. The cycloheximide was used in these experiments to ensure that cytoplasmic GFP-fusion proteins arise from nuclear export and not from new protein synthesis. As a control, we used cells treated only with cycloheximide. After 3 h of treatment, the cells were observed under the fluorescence microscope and the subcellular localization of the GFP-fusion proteins was analyzed as described above.

Cell lysis, immunoprecipitations and western blot analysis

Twenty-four hours after transfection, cells were lysed as previously described (20). The resulting lysates were subjected to either western blotting analysis or immunoprecipitation as described in a previous study (20).

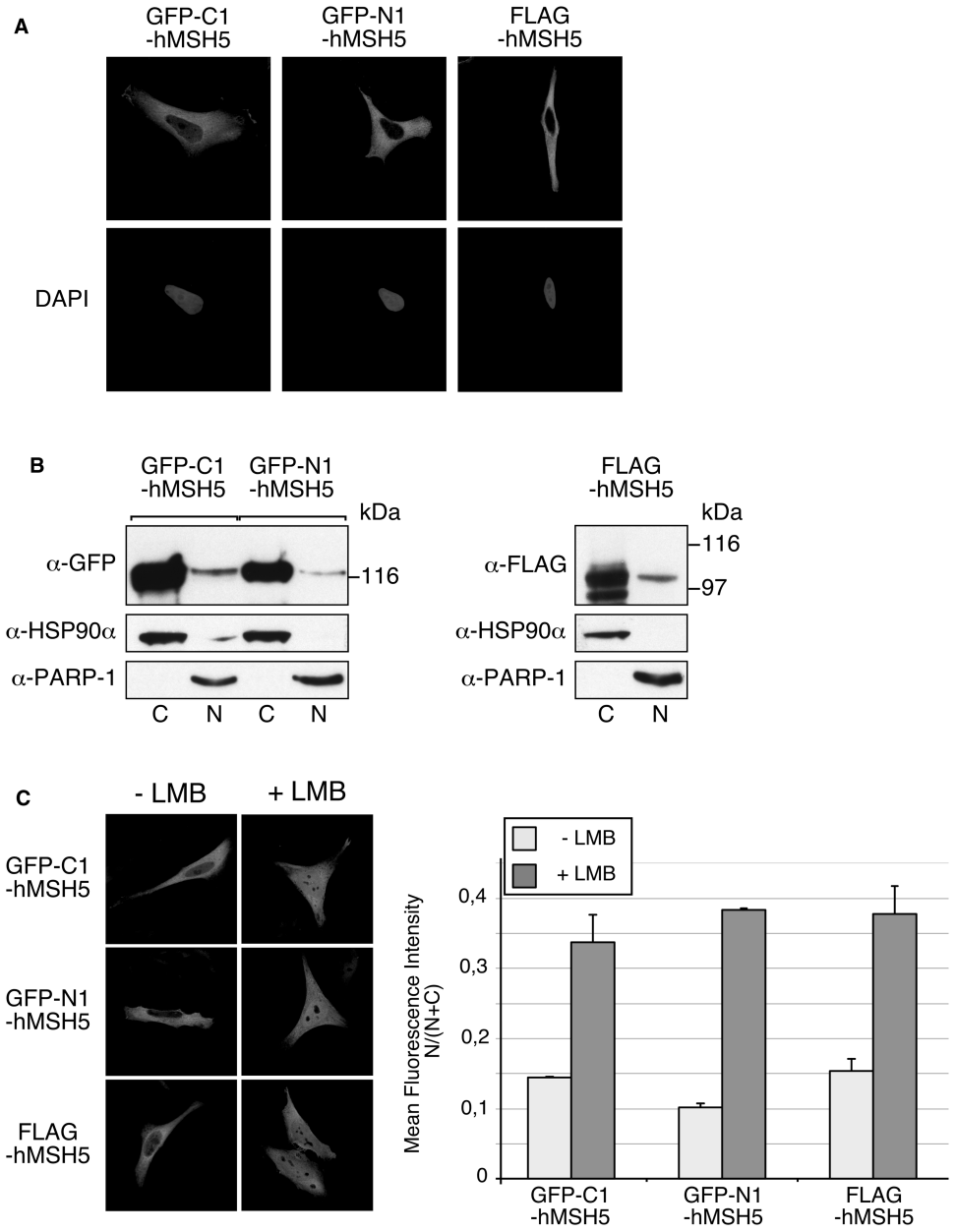

Figure 1. Subcellular distribution of hMSH5 fusion proteins. (**A**) The intracellular distribution of the hMSH5 protein fused to an N-terminal GFP-tag (GFP-C1-hMSH5), a C-terminal GFP-tag (GFP-N1-hMSH5) or an N-terminal FLAG-tag (FLAG-hMSH5) was examined in HeLa cells by laser confocal fluorescence (GFP-tagged proteins) or immunofluorescence (FLAG-hMSH5) microscopy. The images shown are representative of all the transfected cells. Upper panels show the distribution of the indicated fusion protein. Cells were counterstained with DAPI to visualize nuclei (lower panels). (**B**) HeLa cells expressing the indicated proteins were collected and fractionated into cytosolic (C) and nuclear extracts (N). Equal cell amounts from cytosolic and nuclear extracts were immunoblotted with anti-GFP or anti-FLAG antibodies, as indicated. The efficiency of fractionation was verified by staining for HSP90α as a cytoplasmic marker, and PARP-1 as a nuclear marker. (**C**) HeLa cells transiently expressing the indicated fusion proteins were incubated without (–LMB) or with leptomycin B (+LMB) for 6 h. The localization of hMSH5 fusion proteins was determined by fluorescence and immunofluorescence microscopy. Left panels show representative micrographs. The right panel presents a quantitative analysis of the localization data. For each cell, the fluorescence intensities in the entire cell area and in the nuclear area were evaluated, as detailed in 'Material and Methods' section and the nuclear fluorescence was calculated as a percentage of total (nuclear plus cytoplasmic) cell fluorescence (N/N+C). As many as 30–35 cells were analyzed per experiment, for each protein and each condition (±LMB). The graph represents the mean N/N+C values with standard deviations (error bars) across at least three independent experiments.

Subcellular fractionation

Cytosolic and nuclear protein fractions from transfected cells were prepared using the ProteoExtract subcellular proteome extraction kit (Calbiochem), according to the manufacturer's instructions. These fractions were then denaturated in Laemmli sample buffer and equal cellular amounts of each fraction were separated on a 7.5% SDS-polyacrylamide gel and submitted to immunoblotting with the indicated antibodies. The purity and protein content of fractionated extracts were assessed by immunoblotting for

either β-tubulin or HSP90α that localize specifically to the cytoplasmic compartment and for either Lamin B or PARP-1 that are found exclusively in the nuclear compartment.

RESULTS

hMSH5 subcellular distribution is leptomycin B sensitive

We have previously shown that the GFP-hMSH5 fusion protein (also called GFP-C1-hMSH5 herein) is mainly cytoplasmic, and that its subcellular localization is sensitive to leptomycin B (LMB), a specific inhibitor of CRM1-dependent nuclear export (20). To further explore these observations and to exclude the possibility that the intracellular distribution of hMSH5 has been affected by N-terminal GFP tagging, we analyzed by fluorescence microscopy the subcellular localization of hMSH5 fused either to a C-terminal GFP tag (GFP-N1-hMSH5) or to an N-terminal tag consisting of three FLAG octapeptides (FLAG-hMSH5). This was done in transfected HeLa cells (Figure 1A), U2OS cells and WI38 human primary fibroblats (data not shown). Both GFP-N1-hMSH5 and FLAG-hMSH5 appeared to localize predominantly within the cytoplasmic compartment and exhibited a subcellular distribution similar to that of GFP-C1-hMSH5. These observations were confirmed by western blot analysis of fractionated cell lysates of HeLa cells expressing the various hMSH5 fusion proteins (Figure 1B). Similar to GFP-C1-hMSH5, both GFP-N1-hMSH5 and FLAG-hMSH5 underwent nuclear accumulation following leptomycin B treatment of transfected HeLa cells (Figure 1C). Quantification of the nuclear localization of the hMSH5 fusion proteins further showed that GFP-C1-hMSH5, GFP-N1-hMSH5 and FLAG-hMSH5 accumulated in the nucleus to similar extents, upon LMB addition.

These data confirmed that inhibition of the CRM1 transport pathway results in a partial relocalization of hMSH5 when expressed in somatic cells. In addition, they suggested that neither the nature of the tag nor its position at the N- or C-terminus has an effect on hMSH5 nucleocytoplasmic distribution and relocalization in response to LMB. This indicated that the fusion proteins described above could be used to identify potential localization signals in hMSH5 required for its nuclear export and import.

The C-terminal part of hMSH5 exhibits a nuclear export activity

These results prompted us to search whether hMSH5 possesses sequences mediating CRM1-dependent nuclear export. CRM1 recognizes its cargo proteins by binding directly to NESs composed of a short sequence containing regularly spaced leucine or other large hydrophobic amino acids (30). hMSH5 contains several leucine-rich sequences which conform more or less to the NES consensus Φ-x_{2-3}-Φ-x_{2-3}-Φ-x-Φ (where Φ is L, I, V, F or M, and x is any residue) (20). To address the potential contribution of these sequences to hMSH5 nuclear export, deletion constructs were generated as GFP-fused forms (Figure 2A). The resulting GFP-hMSH5 truncated proteins were analyzed by western blot analysis, all of them exhibited the expected size (Figure 2B). We then examined their subcellular distribution and their behavior upon LMB treatment (Figure 2C). The level of nuclear localization (N/N + C ratio) was determined for each truncation mutant, as described in 'Material and Methods' section (Figure 2D).

We first observed that the GFP-hMSH5-[1–524] (also termed Δ1) and GFP-hMSH5-[522–834] (or Δ2) mutants were able to enter the nucleus, suggesting that domains involved in hMSH5 nuclear import are present in the N- and C-terminal half of the protein. We then noticed that the Δ2 mutant was mainly cytoplasmic in the absence of LMB treatment and that it accumulated in the nucleus of HeLa cells to the same extent as the wild-type protein after addition of LMB. By contrast, the Δ1 mutant was markedly more nuclear than the wild type protein and mostly unperturbed by LMB treatment. The behavior of these two mutants suggested that the N-terminal half of the hMSH5 protein does not exhibit a nuclear export activity and that domains involved in CRM1 dependent nuclear export of hMSH5 are located between residues 522 and 834. The truncation GFP-hMSH5-[1–793] (or Δ3) mutant accumulated in the nucleus to a higher extent than the full-length protein and was poorly responsive to LMB treatment. These results further suggested that a nuclear export activity resides within the last 41 amino acids of hMSH5.

Identification of a conserved NES within the C-terminus of hMSH5

Visual examination of the C-terminal amino acid sequence of hMSH5 (794–834 aa) revealed a cluster of hydrophobic residues (802-LVDKFMKLDL-811), conserved among vertebrates and in *Arabidopsis thaliana*, that perfectly matches the NES consensus sequence (Figure 3A). Moreover, the NetNES 1.1 prediction program (31) identified L811, L816 and L818 as residues potentially involved in a nuclear export activity (Figure 3A). These observations prompted us to perform site-directed mutagenesis of one, two or four bulky hydrophobic residues located between aa 802 and aa 818, in the context of the full-length hMSH5 protein (Figure 3B). It is expected that inactivation of a NES results in increased nuclear localization and loss of responsiveness to LMB treatment. The expression of the various GFP-hMSH5 mutants in HeLa transfected cells was evaluated by western blot analysis (Supplementary Figure S1) and their subcellular distribution was analyzed (Figure. 3C). We noticed that alanine replacement of both L816 and L818 (M1 mutant) was without effect on the nucleocytoplasmic distribution pattern of hMSH5. By contrast, converting the leucine 802 to alanine led to a slight but significant nuclear enrichment of the resulting M2 mutant compare with the wild-type protein. A more important increase in nuclear localization was observed when F806, L809 or L811 was mutated to alanine (M3 to M5 mutants, respectively). The mutation of both L809 and L811 (M6 mutant) or of all large hydrophobic

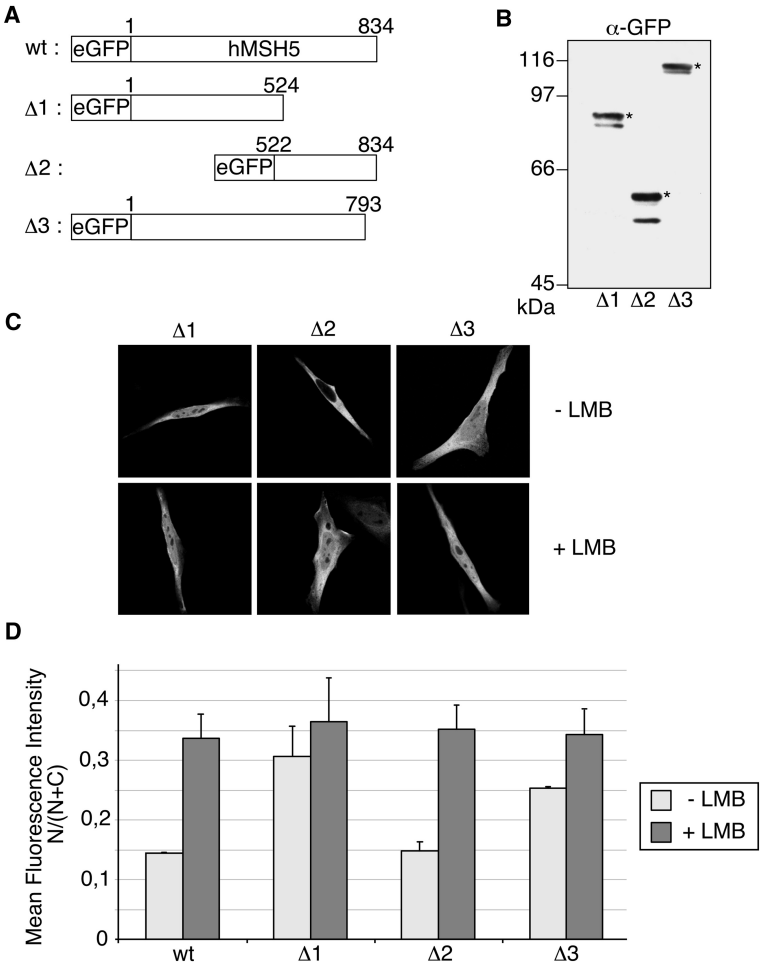

Figure 2. Mapping of hMSH5 regions that exhibit a nuclear export activity. (**A**) Protein structures of the GFP-hMSH5 full-length protein and of the GFP-hMSH5 deletion mutants (Δ1 to Δ3) are shown. Numbers indicate the amino acid number of hMSH5. (**B**) Lysates from HeLa cells transfected with the indicated deletion constructs were analyzed by western blotting with anti-GFP antibodies. Truncated fusion proteins of expected size are marked by a star. (**C**) Representative fluorescence microscopy images of HeLa cells expressing one of the indicated deletion mutant and treated or not with LMB. (**D**) Quantitative analysis of the localization data of the GFP-hMSH5 protein (wt) and of the indicated truncated fusion proteins. The graph shows the mean N/N+C values and standard deviations based on three independent experiments (30–35 cells per experiment were scored).

residues located between aa 802 and 811 (M7 mutant) did not further enhance the nuclear accumulation. Taken together, these observations suggested that the 802-LVDKFMKLDL-811 motif is a functional NES and that residues L802, F806, L809 and L811 contribute to its nuclear export activity. To confirm that these conserved hydrophobic amino acids are involved in CRM1-dependent nuclear export of hMSH5, we examined the subcellular localization of the various GFP-hMSH5 mutants after LMB treatment (Supplementary Figure S2). We then calculated, for the wild-type protein and for each mutant (M1–M7), the fold accumulation in the nucleus induced by LMB as the ratio [N/N+C (+LMB)]/[N/N+C (−LMB)] (Figure 3D). As expected, the M1 mutant exhibited the same sensitivity to LMB treatment as the wild-type protein, while mutations of hydrophobic residues within the 802–811-aa domain rendered the resulting mutants less responsive to LMB. In particular, LMB had only a slight effect on the intracellular distribution of the M7 mutant in which all the hydrophobic amino acids of the NES have been converted to alanine. These data suggested that hMSH5 802–811-aa domain is a functional leucine-rich NES required for CRM1-dependent nuclear export of hMSH5.

The hMSH5 NES exhibits an export activity in an *in vivo* nuclear export assay

We next assessed whether the hMSH5 NES could confer export when fused to other proteins, by using a transfection-based *in vivo* nuclear export assay (24). This assay consists of analyzing the intracellular distribution of the HIV Rev(1.4) protein fused to the GFP, by fluorescence microscopy. While the Rev wild-type protein shuttles between the nucleus and the cytosol owing to its strong NLS and NES, Rev(1.4) is deficient in nuclear export (32). Potential NES sequences can be inserted into the the pRev(1.4)-GFP vector, in order to examine their capability to restor nuclear export activity (Figure 4A). Actinomycin D (ActD) treatment prevents nuclear import of the Rev protein and results in

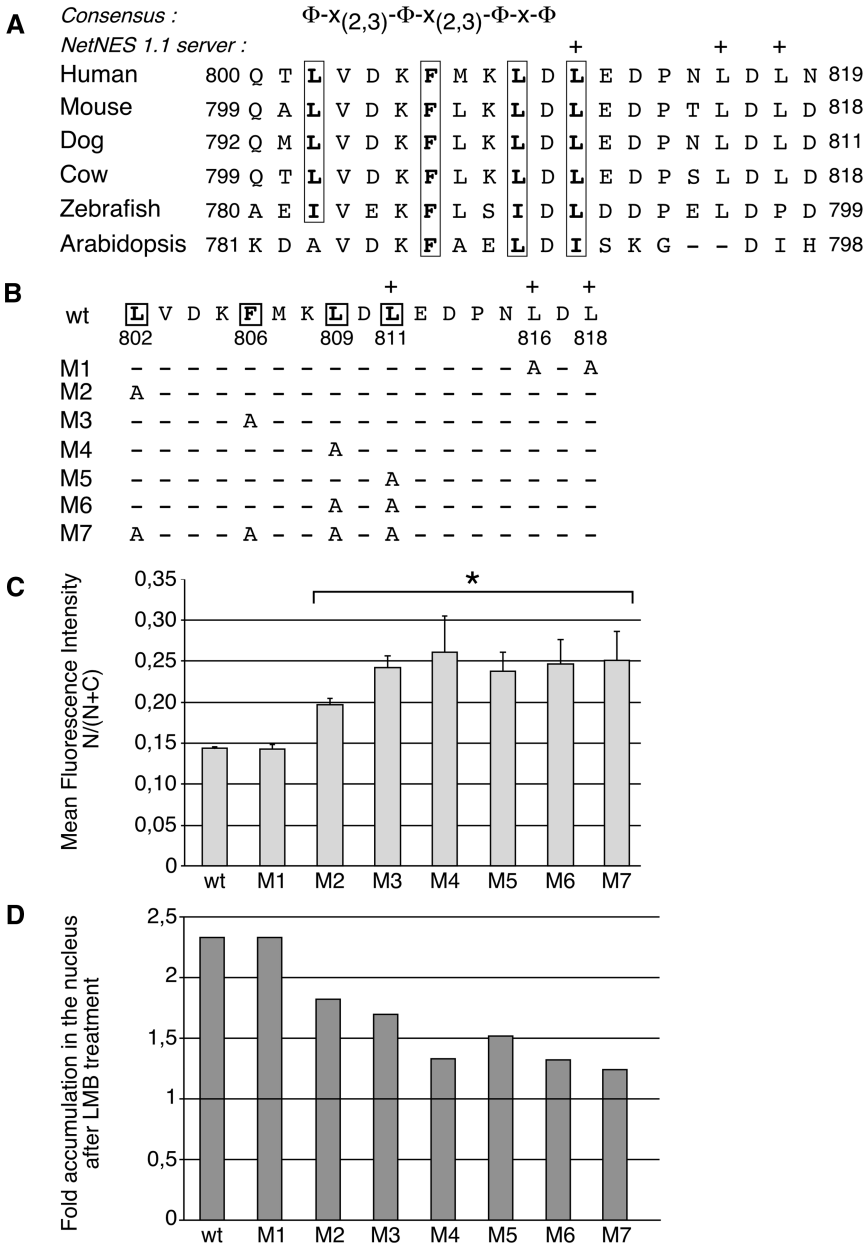

Figure 3. Mutational analysis of the putative hMSH5 NES. (**A**) The NES consensus is shown where Φ represents hydrophobic residues (L, I, F, V, M) and *x* represents any amino acid. Alignment of the putative hMSH5 NES domain with those of other species is shown. Sequences are based on the following accession numbers in GenBank: BAB63375 (*Homo sapiens*), AAD52102 (*Mus musculus*), XP-532080 (*Canis familiaris*), XP-001789888 (*Bos Taurus*), XP-698552 (*Dario rerio*), ABO69626 (*Arabidopsis thaliana*). Residues that fit the NES consensus are boxed, those predicted to be involved in the nuclear export activity by the NetNES 1.1 software are marked by a +. (**B**) Amino acids of hMSH5 NES region that were replaced with alanine are shown. The names of the resulting mutated proteins are indicated (M1–M7). (**C**) Quantitative analysis of the localization data of the wild-type GFP-hMSH5 protein (wt) and the mutants (M1–M7). HeLa cells expressing either GFP-hMSH5 or one of the mutated proteins were examined by fluorescence microscopy. The graph represents the mean N/N + C values with standard deviations of three independent experiments. *P*-values were estimated using a *t*-test and represent the comparison of mean nuclear fluorescence values between each mutant and the wild-type protein. $*P < 0.001$. (**D**) The bar graph shows the fold increase of nuclear localization induced by LMB for the wild-type hMSH5 protein and each mutant.

cytoplasmic accumulation of NES-containing Rev proteins. Consequently, the use of this drug allows the activity of very weak NESs to be detected and the relative activity of different NES can be evaluated by their capability to induce a shift of the GFP signal into the cytoplasm, in the presence (without ActD treatment) or in the absence (with ActD treatment) of active nuclear import. Moreover, if the tested NES is recognized by the CRM1 exportin, the cytoplasmic accumulation of the fusion protein is expected to be inhibited by LMB.

When the wild-type Rev NES is inserted into pRev(1.4)-GFP, the export activity is restored to the Rev wild-type level (24). Therefore, Rev(1.4)-NES-GFP was used as a positive control for nuclear export in our experiments,

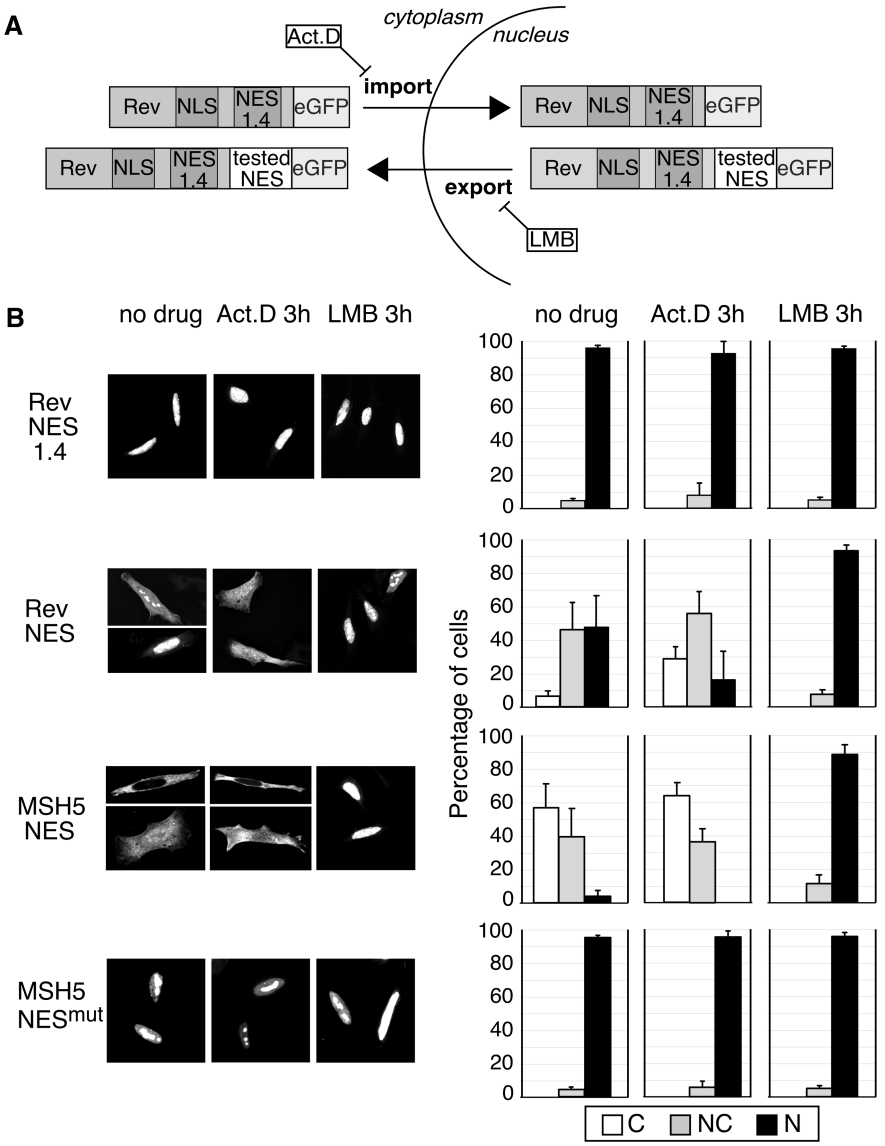

Figure 4. Analysis of the hMSH5 NES activity by using an *in vivo* nuclear export assay. (**A**) Schematic diagram illustrating the basis of the assay to evaluate the activity of a potential NES. (**B**) HeLa cells were transfected with either pRev-1.4-GFP (Rev NES 1.4), pRev-NES-GFP (Rev NES), pRev-MSH5NES-GFP (MSH5 NES) or pRev-MSH5NES^{mut}-GFP (MSH5 NES^{mut}). The subcellular localization of the various fusion proteins, in cells treated with the indicated drug conditions, was analyzed by fluorescence microscopy. Left panels show representative images. Right panels show histograms presenting the percentage of cells for each condition that exhibit only cytoplasmic (C), nuclear plus cytoplasmic (NC) or exclusively nuclear (N), GFP fluorescence staining. Approximately 200 cells were scored for each transfection experiment. The data represent mean values of three independent experiments with standard deviations.

while Rev(1.4)-GFP was the negative control. The wild-type hMSH5 NES and the hMSH5 NES with mutations on residues L802, F806, L809 and L811 were inserted in the pRev(1.4)-GFP plasmid, producing pRev(1.4)-MSH5NES-GFP and pRev(1.4)-MSH5NES^{mut}-GFP, respectively. The subcellular distribution of Rev(1.4)-GFP, Rev(1.4)-NES-GFP, Rev(1.4)-MSH5NES-GFP or Rev(1.4)-MSH5NES^{mut}-GFP was analyzed as described in 'Material and Methods' section. Representative fluorescence images and quantitative data are shown in Figure 4B. As expected, Rev(1.4)-GFP was found exclusively in the nucleus in >90% of cells whatever the drug treatment. The insertion of the Rev wild-type NES sequence resulted in a partial cytoplasmic accumulation of the fusion protein and this tendency was further enhanced after addition of actinomycin D, as previously described (24). We noticed that the insertion of the hMSH5 NES shifted the GFP signal completely to the cytoplasm in more than 55% of cells, even in the absence of actimomycin D and that inhibition of nuclear import only slightly enhanced the percentage of cells exhibiting exclusive cytoplasmic GFP staining (56% without ActD versus 63% after ActD treatment). It has been previously proposed that such a behavior is characteristic of very active NES (24). Therefore, our data raised the possibility that the hMSH5 NES is able to display a strong nuclear export activity. LMB treatment completely inhibited the

activity of the MSH5 NES, confirming that CRM1 is the nuclear receptor for hMSH5. As an additional control, we examined the subcellular distribution of the Rev(1.4)-MSH5NES^{mut}-GFP protein. The fluorescent pattern of this fusion protein was similar to that of the negative control Rev(1.4)–GFP, which confirmed that the 802–811-aa domain of hMSH5 possesses a nuclear export activity that depends on the four conserved 802, 806, 809 and 811 residues.

hMSH5 possesses a weak classical monopartite NLS

We then attempted to identify the regulatory domains involved in the nuclear targeting of hMSH5. The best-characterized nuclear import signals comprise one or two short stretches of basic amino acids and are referred to as classical NLSs. Computer analysis of the hMSH5 sequence with the PSORTII program identified the sequence KKRR (aa 406–409) as a putative NLS. This monopartite cluster of basic amino acid residues is conserved among vertebrates as can be seen in a cross-species comparison of MSH5 amino acid sequence (Figure 5A). Visual and computer-assisted analysis failed to identify other classical NLS within hMSH5. However, it is noteworthy that there are a number of experimentally defined NLSs that do not match the consensus sequence of classical NLS (33). In order to evaluate the potential nuclear import function of the hMSH5 406-KKRR-409 motif and to search for potential non-classical nuclear targeting signals within hMSH5, experiments were performed using an established nuclear transport assay (25). A fragment encoding the putative hMSH5 classical (hMSH5-[404–411]) and fragments spanning the entire open-reading frame of hMSH5 were inserted into the NLS mapping vector pHM830. This vector allows the expression of protein fragments fused both to the GFP and the β-galactosidase proteins (Figure 5B). The GFP functions as a fluorescent tag, while the β-galactosidase increases the molecular weight of the resulting fusion proteins, ensuring that they cannot passively diffuse into the nucleus. The GFP-βgal fusion protein without inserted NLS exhibits a cytoplasmic staining (25) (Figure 5C and D). By contrast, the GFP-βgal fusion protein containing the NLS of SV40 LT is known to be localized almost exclusively in the nucleus (25) and was used in our experiments as a positive control for nuclear targeting (Figure 5C and D). The localization of the various fusion proteins was examined by fluorescence microscopy (Figure 5C and D). As expected, the GFP-βgal protein was exclusively cytoplasmic in more than 80% of transfected cells. Insertion of hMSH5-[404–411] fragment was found to enhance the nuclear localization of the resulting fusion protein, albeit to a lower extent than the insertion of SV40 LT NLS. These data indicated that the hMSH5-[404–411] domain allows the targeting of a heterologous protein to the nucleus, suggesting that 406-KKRR-409 motif is a functional NLS. Our observation also suggested that this hMSH5 NLS exhibits a weak nuclear import activity compared with SV40 LT NLS. None of the other hMSH5 protein fragments was able to translocate the corresponding fusion proteins to the nucleus (Figure 5C and D). As the hMSH5-[700–834] segment includes the NES domain, the subcellular localization of GFP-hMSH5-[700–834]-βgal was examined before and after inhibition of nuclear export by LMB, in order to test the possibility that the hMSH5 NES has overcome the activity of a potential NLS. This fusion protein was almost exclusively cytoplasmic in both conditions (Figure 5C and D), suggesting that the hMSH5-[700–834] fragment does not contain a NLS. Taken together, these results supported the view that hMSH5 does not contain nuclear targeting signal other than the 406-KKRR-409 motif. However, this seemed unlikely since GFP-hMSH5-[522–834] has the capability to enter the nucleus (Figure 2). One possible explanation for these contradictory observations is that one or several of the GFP-hMSH5-βgal fusion products adopt folded conformations that compromise the accessibility of potential hMSH5 domains to either members of the importin superfamily transporters or NLS-containing partners.

In order to test whether the 406-KKRR-409 motif participates to the nuclear targeting of hMSH5, site-directed mutagenesis was performed to substitute lysine and arginine with alanine in the context of the full-length hMSH5 protein (Figure 6A). The expression of resulting mutated proteins was assessed by western blot analysis (Figure 6B) and their subcellular distribution was analyzed by confocal fluorescence microscopy (Figure 6C). Mutations in the NLS of hMSH5 did not significantly reduce the nuclear localization of the resulting mutated proteins, when compared with the wild-type (percentage of nuclear localization, wt: $14.4 \pm 0.03\%$; m8: $11.1 \pm 0.81\%$; m9: $11.09 \pm 1.72\%$; m10: $11.74 \pm 0.96\%$). We reasoned that a reduction of the nuclear activity of hMSH5 NLS motif might not be detected without inhibiting hMSH5 nuclear export. Therefore, we analyzed the subcellular localization of the three NLS-mutated GFP-hMSH5 proteins after LMB treatment (Figure 6C). GFP-hMSH5 proteins bearing mutations in the NLS motif accumulated in the nucleus to a significant lesser extent than the wild-type protein after LMB treatment, which indicated that the nuclear import of these NLS-mutants is altered. Converting all the basic amino acids within the NLS to alanine led to a further significant decrease in the nuclear localization of the corresponding m10 mutant when compared with m8 and m9 mutants, after inhibition of the nuclear export. These findings suggested that 406-KKRR-409 motif acts as a true nuclear localization signal in the context of the hMSH5 protein and that both pairs of basic amino acids within this NLS (406 K/407 K and 408 R/409 R) contribute to its nuclear export activity. We also observed that the addition of LMB induced a slight but significant nuclear enrichment of the m10 mutant, suggesting that this mutated protein exhibits a residual nuclear import activity. This observation supported the possibility that a nuclear targeting domain other than the above-characterized NLS might contribute to hMSH5 nuclear import, which was consistent with the fact that the GFP-hMSH5-[522–834] truncated mutant is able to enter the nucleus.

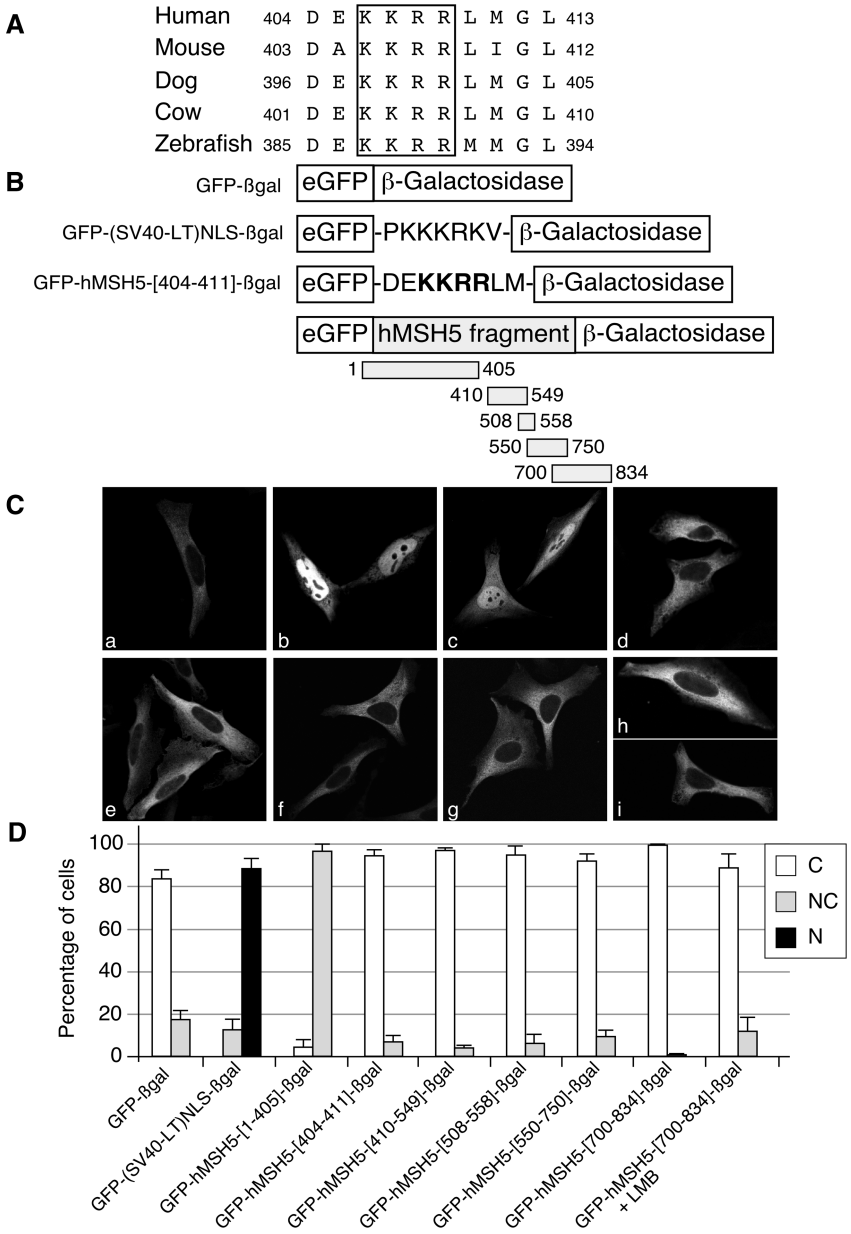

Figure 5. Mapping of putative NLS sites in hMSH5. (**A**) Conservation of the MSH5 NLS sequence (boxed residues) among vertebrates. (**B**) Schematic representation of the GFP-βgal protein encoded by the pHM830 vector and of the various fusion proteins encoded by the pHM830-derived constructs. The basic amino acids within the putative hMSH5 NLS are shown in bold typeface. hMSH5 amino acids at the boundaries of the regions fused to GFP and β-galactosidase are indicated. (**C**) Representative confocal microscopy images of HeLa cells expressing: a, GFP-βgal (negative control); b, GFP-(SV40-LT)NLS-βgal (positive control); c, GFP-hMSH5-[404–411]-βgal; d, GFP-hMSH5-[1–405]-βgal; e, GFP-hMSH5-[410–549]-βgal; f, GFP-hMSH5-[508–558]-βgal; g, GFP-hMSH5-[550–750]-βgal; h, GFP-hMSH5-[700–834]-βgal (without LMB treatment); i) GFP-hMSH5-[700–834]-βgal (plus LMB treatment). (**D**) The percentage of HeLa cells displaying only cytoplasmic (C), nuclear plus cytoplasmic (NC) or exclusively nuclear (N) GFP staining was determined for the indicated proteins. For each protein, approximately 200 cells were counted per experiment. Values shown in the bar graph are the means of three independent experiments with standard deviations.

Proteasomal degradation restricts the nuclear life span of hMSH5

The above data suggested that hMSH5 is a nucleocytoplasmic shuttling protein exported from the nucleus through the CRM1 pathway. It is known for several proteins that nuclear export is a prerequisite for their degradation (34–36). As a first step toward investigating whether hMSH5 follows a similar fate, we examined the relationship between its subcellular localization and its stability. HeLa cells expressing GFP-hMSH5 were treated with cycloheximide to inhibit *de novo* protein synthesis or with DMSO as a control. Nuclear and cytoplasmic fractions were prepared at the indicated time points and analyzed by immunoblotting to assess GFP-hMSH5 levels (Figure 7A). The amount of cytoplasmic and nuclear GFP-hMSH5 was not affected by DMSO. The level of the cytoplasmic GFP-hMSH5 declined by ~25% 2 h after addition of

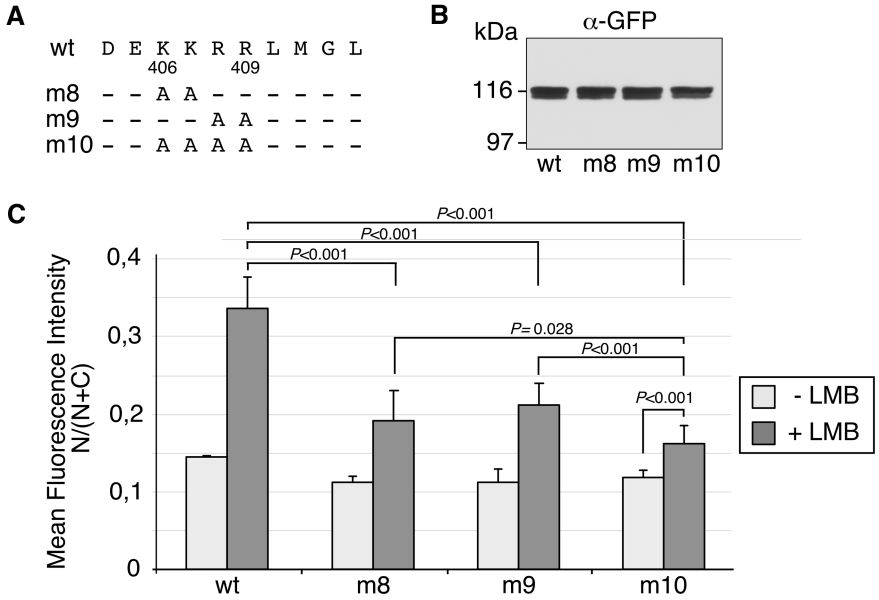

Figure 6. Site-directed mutagenesis of the putative hMSH5 classical monopartite NLS. (**A**) Amino acids of the hMSH5 NLS that were replaced with alanine are shown. The names of the resulting mutants are indicated (m8–m10). (**B**) Lysates from HeLa cells expressing the indicated mutated protein were analyzed by western blotting with anti-GFP antibodies. (**C**) Quantitative analysis of the subcellular localization of hMSH5 NLS-mutated fusion proteins. HeLa cells expressing the indicated GFP fusion proteins were treated or not with LMB before fixation, and examined by confocal fluorescence microscopy. For each cell, the fluorescence intensities were measured in the entire cell and in the nuclear area, in order to calculate the N/N + C ratio. As many as 30–35 cells were analyzed per experiment, for each construct and each incubation condition (± LMB). The graph shows the mean N/N + C values with standard deviations across three independent experiments. Statistically significant *P*-values are indicated.

cycloheximide, while the same treatment resulted in a 75% reduction of the nuclear GFP-hMSH5 (Figure 7A and B). These data suggested that hMSH5 stability depends on its subcellular localization and that nuclear localization is linked with increased destabilization. Degradation of most cellular proteins proceeds via an energy-dependent process involving the 26S proteasome that constitutes the major proteolytic activity in both the cytosol and the nucleus. Therefore, we examined the effect of the 26S proteasome inhibitor MG132 on the turnover of GFP-hMSH5 in both compartments. HeLa transfected cells were treated with a combination of cycloheximide and MG132 before analysis of GFP-hMSH5 levels (Figure 7A and B). The inhibition of the proteasome resulted in a stabilization of the tagged hMSH5 protein in both the cytoplasm and the nucleus (Figure 7A and B), suggesting that both cytoplasmic and nuclear proteasome can target hMSH5 for degradation.

These data supported the view that CRM1-dependent nuclear export is not required for hMSH5 efficient degradation. On the contrary, they rather suggested that forcing localization of hMSH5 within the nucleus would enhance its destabilization. To verify this hypothesis, transfected HeLa cells were mock-treated or incubated with LMB, 4 h prior to the addition of either cycloheximide or DMSO. Two hours later, cells were collected and GFP-hMSH5 levels were subsequently examined (Figure 7C). Approximately 62 ± 2.9% of the protein were degraded after cycloheximide treatment when the cells have been pre-incubated with LMB, while only 23 ± 11% of degradation was observed without LMB pre-treatment. These observations further supported that nuclear hMSH5 is much less stable than the cytoplasmic protein and thereby confirmed that the CRM1 nuclear export does not favor hMSH5 degradation.

The hMSH5 NLS activity and the masking of the hMSH5 NES are both involved in determining the subcellular localization of the hMSH4-hMSH5 complex

Although emerging data indicate that MSH5 can function independently of MSH4, this MutS homolog is primarily known to function as a heterodimer with MSH4. Therefore, we have previously investigated the consequences of the interaction between hMSH4 and hMSH5 on their subcellular distribution (20). We have found that both hMSH4 and hMSH5 are independently capable to enter and exit the nucleus. Nevertheless, their heterodimerization mutually facilitated their nuclear localization. Some findings have led us to hypothesize that dimerization might partially impair hMSH5 nuclear export on the one hand, and facilitate hMSH4 nuclear import on the other hand (20). To further explore these assumptions, we took advantage of the identification of hMSH5 NES and NLS motifs and attempted to investigate the effect of inactivation of these motifs on the intracellular distribution of the hMSH4-hMSH5 heterodimer. We first tested whether GFP-hMSH5 mutated at the four residues critical for the NES activity (M7 mutant also called GFP-hMSH5-NES^{mut}) or at the four residues required for the NLS functionality (m10 mutant or GFP-hMSH5-NLS^{mut}) was still able to interact with hMSH4 (Figure 8A). The wild-type GFP-hMSH5 protein and a deletion mutant (GFP-hMSH5-[1–524])

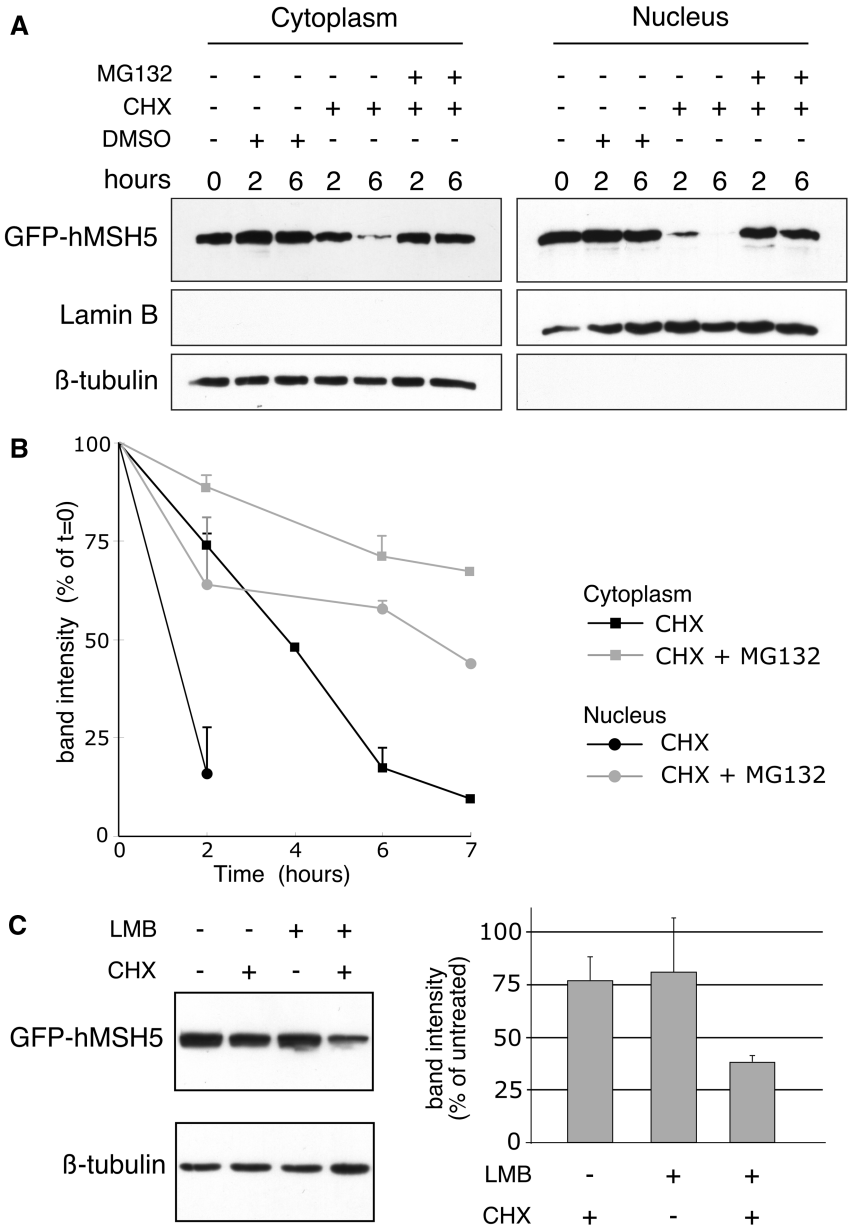

Figure 7. Analysis of hMSH5 stability in both the cytoplasm and the nucleus. (**A**) HeLa cells expressing GFP-hMSH5, were treated with either DMSO, cycloheximide (CHX) or cycloheximide plus MG132. Cells were collected at the indicated time points and subjected to cytoplasmic (left panel) and nuclear (right panel) fractionation. GFP-hMSH5 levels were assessed using immunoblotting with anti-GFP antibodies. Protein loading for cytoplasmic and nuclear samples was normalized by western blot for β-tubulin and Lamin B, respectively. β-Tubulin and Lamin B also serve as cytoplasmic and nuclear markers, respectively. (**B**) Similar experiments to that presented in (A) were conducted and resulting autoradiographs were subjected to densitometric analysis by using ImageJ software (version 1. 36 b). Cytoplasmic and nuclear GFP-hMSH5 signals were normalized to the β-tubulin or Lamin B signals, respectively and were expressed as percentage of the initial signal (t = 0 h). The data shown are mean of the results from two to three experiments. (**C**) HeLa cells expressing GFP-hMSH5 were incubated with or without LMB. After 4 h, cells were treated by adding or not cycloheximide for a period of 2 h. A that point, whole cell extracts were prepared and equal amount of the various samples were subjected to western blot analyses with anti-GFP and β-tubulin antibodies (left panels). Densitometric analyses of autoradiographs were performed with ImageJ software. For each condition, GFP-hMSH5 signal was normalized to the β-tubulin signal and was expressed as percentage of untreated signal. The mean percentages of normalized GFP-hMSH5 levels with standard deviations across three independent experiments are presented as a bar graph (right panel).

that lacks the C-terminal hMSH4 interaction domain (10,20) were also used in interaction assays as positive and negative control, respectively. Extracts from HeLa cells, co-expressing the DsRed-hMSH4 protein with either GFP-hMSH5, GFP-hMSH5-[1–524], GFP-hMSH5-NES^{mut} or GFP-hMSH5-NLS^{mut}, were subjected to immunoprecipitation with anti-GFP antibodies (Figure 8A). As expected, the GFP-hMSH5 and DsRed-hMSH4 proteins were associated in HeLa cells whereas GFP-hMSH5-[1–524] and DsRed-hMSH4 did not appear to interact with one another. Interestingly, mutations of the four consensus residues in the hMSH5 NES were sufficient to abolish or, at least, strongly affect the association between hMSH4 and hMSH5 in our assay.

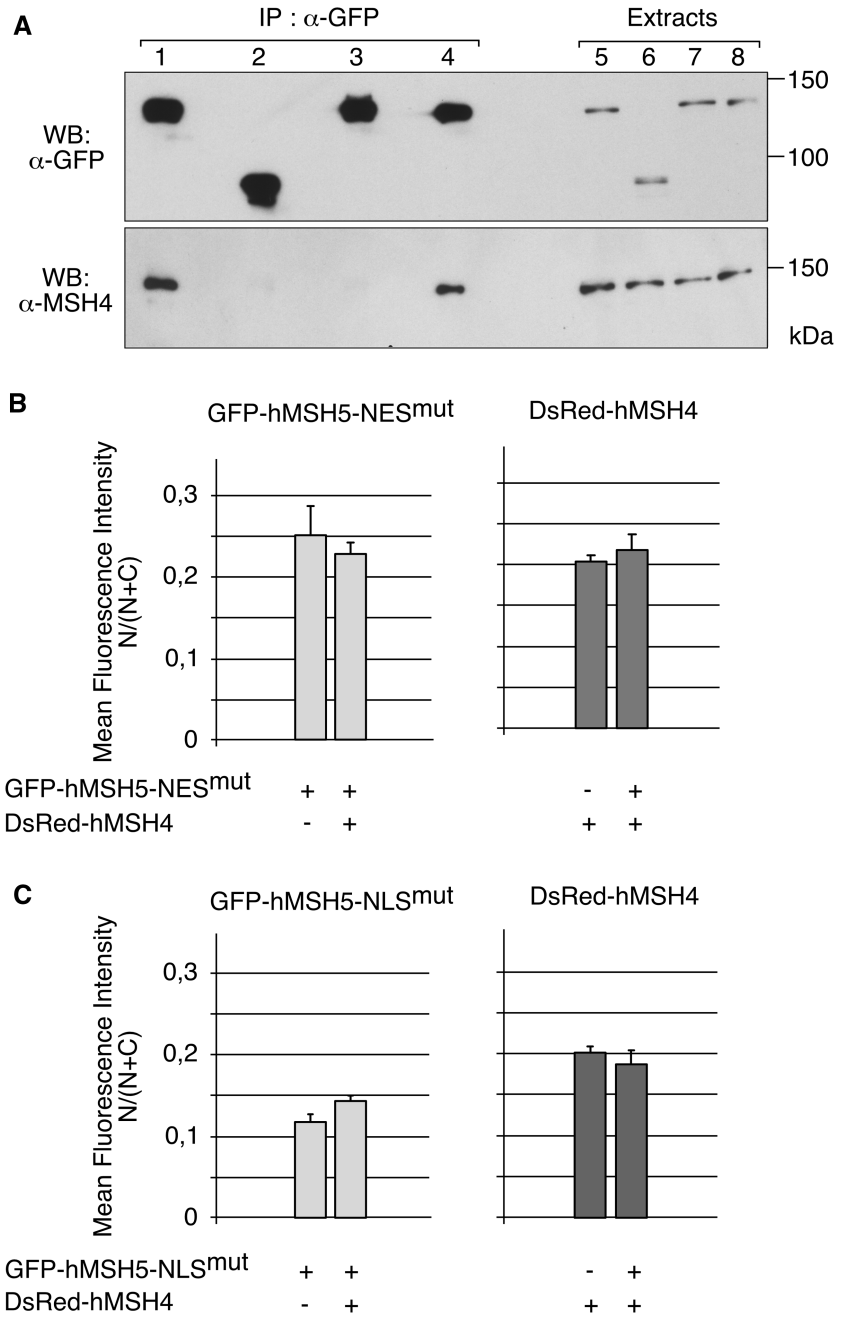

Figure 8. Analysis of the subcellular localization of the NES and NLS-mutated hMSH5 proteins when co-expressed with hMSH4. (**A**) Protein extracts from HeLa cells co-expressing DsRed-hMSH4 with either GFP-hMSH5 (lanes 1 and 5), GFP-hMSH5-[1–524] (87 kDa) (lanes 2 and 6), GFP-hMSH5-NES^{mut} (lanes 3 and 7) or GFP-hMSH5-NLS^{mut} (lanes 4 and 8) were submitted to immunoprecipitation with anti-GFP antibodies (lanes 1–4) or directly analyzed by immunoblotting, as a control (lanes 5–8). Immunoprecipitates and extracts were immunoblotted with anti-GFP or anti-MSH4 antibodies (20), as indicated. (**B**) The subcellular localization of GFP-hMSH5-NES^{mut} (left panel) and DsRed-hMSH4 (right panel) was quantitatively analyzed when these proteins were expressed either alone or together in HeLa cells. The graphs represent N/N + C mean values, calculated as described in 'Material and Methods' section and in Figure 1 legend, with standard deviations from three independent experiments. (**C**) The same analyses were performed for GFP-hMSH5-NLS^{mut} (left panel) and DsRed-hMSH4 (right panel) expressed either alone or together in HeLa cells.

By contrast, interaction between hMSH4 and hMSH5 appeared unaffected by mutagenesis of the hMSH5 NLS. These interaction data are consistent with the fact that hMSH5 NES (aa 802–811) is located within the hMSH4-binding domain (aa 731–833), unlike the hMSH5 NLS (aa 406–409).

The co-expression and interaction of wild-type hMSH5 and hMSH4 proteins in HeLa cells have been shown to result in a significant nuclear enrichment of both of them (20). Here, we observed that the subcellular distribution of GFP-hMSH5-NES^{mut} (Figure 8B, left panel) and DsRed-hMSH4 (Figure 8B, right panel) was not

significantly modified upon their co-expression, which was consistent with interaction data (Figure 8A). We concluded that some or all of the amino acids required for hMSH5 nuclear export are also critical for the binding of hMSH4. This finding implied that hMSH4 binding could interfere with the accessibility of the hMSH5 NES to the export machinery, and thus was consistent with the fact that hMSH5 is less sensitive to LMB when bound to hMSH4 (20).

Although the NLS-mutated hMSH5 protein has retained its capacity to interact with hMSH4, the nuclear localization of GFP-hMSH5-NLS^{mut} remained almost unchanged when expressed alone or with DsRed-hMSH4 (Figure 8C, left panel). The nuclear localization of DsRed-hMSH4 was not increased upon co-expression with GFP-hMSH5-NLS^{mut} (Figure 8C, right panel), whereas it is significantly increased upon co-expression with the wild-type GFP-hMSH5 protein (20). These observations suggested that the hMSH5 NLS is required for the maximal nuclear localization of the hMSH4-hMSH5 heterodimer.

Together, these data led us to propose that two important parameters that play a role in determining the nuclear localization of the hMSH4-hMSH5 complex are the reduction of hMSH5 nuclear export upon heterodimerization and the nuclear targeting activity of the hMSH5 NLS.

DISCUSSION

Recent findings strongly support the premise that in addition to its role in meiotic recombination, hMSH5 is involved in different cellular processes and that dimerization with hMSH4 is probably not required for all of its functions. It has been proposed that hMSH5 participates in mitotic DNA recombination and DNA damage signaling (4). Hence, appropriate regulation of hMSH5 activity may play a critical role in genomic stability. As a first step toward analyzing the mechanisms involved in the control of hMSH5 activity, we investigated its cellular trafficking properties. We determined that hMSH5 is a nucleocytoplasmic shuttling protein that can actively enter and exit the nucleus. In agreement with previous data (20), exogenously expressed hMSH5 was predominantly observed in the cytoplasm. However, upon inhibition of the CRM1-mediated nuclear export pathway, hMSH5 accumulated in the nucleus of transiently (Figure 1) or stably transfected cells (Supplementary Figure S3). Moreover, various truncated hMSH5 fusion proteins, expressed at a level comparable to the GFP-hMSH5 wild-type protein (data not shown), exhibited subcellular distribution and LMB sensitivity distinct from that of the full-length protein. These observations led us to investigate whether hMSH5 possesses intrinsic signals that direct its intracellular distribution. We identified the hMSH5 sequence ^{802}LVDKFMKLDL^{811} as a functional NES. This conclusion was reached based on three observations. First, the 802–811 sequence perfectly fits the NES consensus. Hydrophobic residues within this sequence are conserved among vertebrates and in the plant *Arabidopsis thaliana,* which suggests a biological significance. Second, the mutation of large hydrophobic amino acids within this motif resulted in significant nuclear accumulation of hMSH5 and rendered the protein much less responsive to LMB treatment (Figure 3 and Supplementary Figure S3). The mutation of both L809 and L811 residues was sufficient to render hMSH5 almost insensitive to LMB. Third, the ^{802}LVDKFMKLDL^{811} sequence was able to mediate nuclear export of an export-defective Rev fusion protein and this effect was abrogated after LMB treatment or after introducing mutations at L802, F806, L809 and L811. It has been shown, by using the Rev(1.4)-GFP nuclear export assay, that different NESs can vary importantly in activity. Nuclear export sequences with low activity, as in Hdm2 and p53, have been shown to increase cytoplasmic GFP staining only in the presence of actinomycin D (24). By contrast, the hMSH5 NES was able to shift GFP staining to the cytoplasm without actinomycin D treatment in more than 55% of cells. Collectively, these data indicate that hMSH5 harbors a functional NES in its C-terminal region that mediates its nuclear export through the CRM1-dependent pathway and they support the possibility that this NES may exert a strong nuclear export activity.

Analysis of the hMSH5 primary sequence revealed a cluster of basic amino acids, ^{406}KKRR^{409}, that was conserved among vertebrates and resembled a classical monopartite NLS. This motif was able to promote nuclear import when fused to a heterologous protein, albeit to a lesser extent than the strong SV40 LT NLS. It was also functional in the context of the hMSH5 full-length protein, as assessed by mutagenesis. Indeed, mutation of the K406/K407 and/or R408/R409 residues pairs affected nuclear accumulation of the corresponding mutated proteins in response to LMB, indicating that the ^{406}KKRR^{409} peptide motif is crucial for hMSH5 nuclear import even though it exhibits weak activity when fused to a heterologous protein (Figure 6 and Supplementary Figure S3). A variety of proteins are known to contain multiple NLSs (37–40), including some containing nonconventional NLSs that do not conform to either classical monopartite or bipartite motifs (41–43). To determine whether this is the case for hMSH5, we assessed the ability of different hMSH5 segments to drive nuclear accumulation of fused GFP-β-galactosidase. Other than the ^{406}KKRR^{409} NLS, we did not identify any additional nuclear targeting sequences. However, the fact that the GFP-hMSH5-[522–834] protein was able to enter the nucleus (Figure 2C) led us to deduce that at least one site is present between amino acids 522 and 834, that is seemingly inaccessible in the context of GFP-β-galactosidase fusion proteins and that corresponds to either a nonclassical NLS or to an interacting domain with a NLS-containing partner. Additional investigations will be necessary to identify this potential nuclear targeting domain and to determine whether it functions independently or cooperatively with the identified NLS in the context of the full-length protein.

LMB treatment did not result in complete nuclear accumulation of hMSH5 (Figure 1 and Supplementary Figure S3). Likewise, ectopically expressed hMSH5 with inactivating mutations in the NES did not fully accumulate in the nucleus (Figure 3 and Supplementary Figure S3). There are several mechanisms that may be responsible for this. A first possibility is that efficient nuclear targeting of hMSH5 requires not only the identified NLS but also NLS-containing partners that may be present in limited amounts relative to the amount of overexpressed hMSH5 fusion protein. A prediction of this assumption is that fusion of a strong heterologous NLS to hMSH5 should rescue nuclear import and enhance hMSH5 nuclear localization, at least after LMB treatment. However, we observed that when expressed in HeLa cells, treated or not by LMB, the GFP-NLS-hMSH5 protein containing the strong SV40 LT NLS was only slightly more nuclear than GFP-hMSH5 (Supplementary Figure S4). In contrast, fusion of this NLS to β-galactosidase or to hMSH4 induced a strong increase in the nuclear localization of the resulting hybrid proteins (Supplementary Figure S4). These results did not support the first possibility. As proteins that utilize both CRM1-dependent and independent nuclear export pathways have been described (44,45), a second hypothesis is that hMSH5 may also be exported from the nucleus through a currently unidentified CRM1-independent pathway. Finally, a third explanation for the subcellular distribution pattern of hMSH5 could be that this protein is sequestered in the cytoplasm by association with either binding partners, organelles or cytoskeletal filaments, as has been described for other proteins (17,46). Further experiments will be required to distinguish between the two latter possibilities. However, these findings provide a basis for the argument that hMSH5 subcellular movements are subject to an intricate level of regulation that is reminiscent of what has been described for other multifunctional proteins, such as p53 or BRCA1 (17,46).

A link between nucleocytoplasmic shuttling and protein degradation has been demonstrated for several molecules. Degradation of most proteins in mammalian cells is carried out by the 26S proteasome, usually after the protein has been tagged with a polyubiquitin chain (47). Although the proteasome system operates in both the cytoplasm and the nucleus (48), export to the cytoplasm appears to be required for efficient degradation of several proteins (35,36,49). We found that nuclear export did not facilitate degradation of hMSH5. Instead, hMSH5 nuclear localization appeared to be associated with increased degradation. This was assessed by analysis of hMSH5 levels in nuclear and cytoplasmic extracts of HeLa cells at different times after treatment with cycloheximide and supported by the finding that impairment of nuclear export with LMB resulted in a decrease in hMSH5 levels in total cell lysates. Degradation of both cytoplasmic and nuclear hMSH5 was reduced by treatment with the proteasome inhibitor MG132. Although ubiquitination of hMSH5 remains to be investigated, these data support the assumption that degradation of hMSH5 occurs via the 26S proteasome, in both cytoplasmic and nuclear compartments, albeit much more rapidly in the nucleus. Precedence for nuclear proteasome-mediated downregulation of proteins (e.g. for p53) has been established (50) and it has been proposed that local nuclear destruction may be crucial for the rapid turn off of nuclear pathways.

Taken together, our findings suggest that both CRM1-dependent nucleocytoplasmic shuttling and proteasomal degradation contribute to limit the level of hMSH5 in the nucleus. Moreover, some of our observations lead us to speculate that additional mechanisms, such as cytoplasmic sequestration and/or CRM1-independent nuclear export, may also be involved in the maintenance of low levels of nuclear hMSH5. The biological significance of the existence of different mechanisms by which to downregulate hMSH5 nuclear content has yet to be determined. As uncontrolled amounts of hMSH5 in the nucleus could be deleterious for genomic stability, multiple means of regulation may be required to prevent hMSH5-dependent DNA transactions. Nuclear-cytoplasmic shuttling is necessary to impede the accumulation of certain proteins in the nucleus but it also plays an essential role in the movement of various proteins between different cellular organelles and structures. In particular, several shuttling proteins involved in DNA damage repair and signaling have been shown to travel between distinct subcellular organelles including the nucleus, mitochondria and centrosome and this intracellular trafficking is thought to be crucial for the cell to provide an appropriate DNA damage response (51). Here, we provide evidence that hMSH5 is a shuttling protein. Whether its intracellular trafficking plays a role in DNA damage signaling and repair is an issue that remains to be addressed.

It appears that hMSH5 could function independently of or in association with hMSH4. Therefore, it is of interest to characterize the intracellular trafficking properties of the hMSH4-hMSH5 heterodimer. Oligomerization-regulated NES/NLS activities have been reported for several proteins (17,52), and we have shown previously that dimerization of hMSH4 and hMSH5 promotes the nuclear localization of both proteins. This may result from enhanced nuclear import and/or less efficient nuclear export of these proteins when they form a complex, since they interact with each other in both cytoplasmic and nuclear compartments (20). Identification of hMSH5 NES and NLS motifs allowed us to gain a better understanding of the mechanisms that underlie the subcellular distribution of the hMSH4-hMSH5 complex. First, the demonstration that the L802, F806, L809 and L811 residues are required for both hMSH5 NES activity and hMSH4 binding further supports the previous assumption that heterodimerization enhances nuclear retention of hMSH5 by masking its NES (20). Second, our finding that mutagenesis of the NLS motif in hMSH5 affects the nuclear localization of the hMSH4-hMSH5 heterodimer is in agreement with the hypothesis that interaction between hMSH5 and hMSH4 might enhance hMSH4 nuclear localization via facilitation of its nuclear import (20). Together, these findings prompt us to propose that the hMSH4-hMSH5 complex translocates to the nucleus via, at least in part, the hMSH5 NLS and that hMSH4 binding affects the

export activity of the hMSH5 NES. Our data also suggest that the hMSH4-hMSH5 heterodimer can still be exported from the nucleus through the hMSH4 NES. Although it remains to be determined how the intracellular trafficking of hMSH4-hMSH5 regulates the function of this complex, we believe that hMSH4 and hMSH5 proteins constitute an interesting model of reciprocal regulation of nuclear transport by dimerization.

SUPPLEMENTARY DATA

Supplementary Data are available at NAR Online.

ACKNOWLEDGEMENTS

We thank Dr Beric Henderson for the generous gifts of the pRev(1.4)-GFP vector and the same vector bearing the Rev nuclear export sequence. We are also grateful to Dr Thomas Stamminger for kindly providing the pHM830 and pHM840 plasmids.

FUNDING

The Centre National de la Recherche Scientifique Electricité de France, conseil de radioprotection (RB 2009-05 to S.S.-D.). Funding for open access charge: The Centre National de la Recherche Scientifique.

Conflict of interest statement. None declared.

REFERENCES

1. de Vries,S.S., Baart,E.B., Dekker,M., Siezen,A., de Rooij,D.G., de Boer,P. and te Riele,H. (1999) Mouse MutS-like protein Msh5 is required for proper chromosome synapsis in male and female meiosis. *Genes Dev.*, **13**, 523–531.
2. Kneitz,B., Cohen,P.E., Avdievich,E., Zhu,L., Kane,M.F., Hou,H. Jr, Kolodner,R.D., Kucherlapati,R., Pollard,J.W. and Edelmann,W. (2000) MutS homolog 4 localization to meiotic chromosomes is required for chromosome pairing during meiosis in male and female mice. *Genes Dev.*, **14**, 1085–1097.
3. Snowden,T., Acharya,S., Butz,C., Berardini,M. and Fishel,R. (2004) hMSH4-hMSH5 recognizes Holliday Junctions and forms a meiosis-specific sliding clamp that embraces homologous chromosomes. *Mol. Cell*, **15**, 437–451.
4. Her,C., Zhao,N., Wu,X. and Tompkins,J.D. (2007) MutS homologues hMSH4 and hMSH5: diverse functional implications in humans. *Front. Biosci.*, **12**, 905–911.
5. Paquis-Flucklinger,V., Santucci-Darmanin,S., Paul,R., Saunieres,A., Turc-Carel,C. and Desnuelle,C. (1997) Cloning and expression analysis of a meiosis-specific MutS homolog: the human MSH4 gene. *Genomics*, **44**, 188–194.
6. Winand,N.J., Panzer,J.A. and Kolodner,R.D. (1998) Cloning and characterization of the human and Caenorhabditis elegans homologs of the Saccharomyces cerevisiae MSH5 gene. *Genomics*, **53**, 69–80.
7. Her,C. and Doggett,N.A. (1998) Cloning, structural characterization, and chromosomal localization of the human orthologue of Saccharomyces cerevisiae MSH5 gene. *Genomics*, **52**, 50–61.
8. Bocker,T., Barusevicius,A., Snowden,T., Rasio,D., Guerrette,S., Robbins,D., Schmidt,C., Burczak,J., Croce,C.M., Copeland,T. *et al.* (1999) hMSH5: a human MutS homologue that forms a novel heterodimer with hMSH4 and is expressed during spermatogenesis. *Cancer Res.*, **59**, 816–822.
9. Her,C., Wu,X., Griswold,M.D. and Zhou,F. (2003) Human MutS homologue MSH4 physically interacts with von Hippel–Lindau tumor suppressor-binding protein 1. *Cancer Res.*, **63**, 865–872.
10. Yi,W., Wu,X., Lee,T.H., Doggett,N.A. and Her,C. (2005) Two variants of MutS homolog hMSH5: prevalence in humans and effects on protein interaction. *Biochem. Biophys. Res. Commun.*, **332**, 524–532.
11. Geissler,S., Siegers,K. and Schiebel,E. (1998) A novel protein complex promoting formation of functional alpha- and gamma-tubulin. *EMBO J.*, **17**, 952–966.
12. Yi,W., Lee,T.H., Tompkins,J.D., Zhu,F., Wu,X. and Her,C. (2006) Physical and functional interaction between hMSH5 and c-Abl. *Cancer Res.*, **66**, 151–158.
13. Tompkins,J.D., Wu,X., Chu,Y.L. and Her,C. (2009) Evidence for a direct involvement of hMSH5 in promoting ionizing radiation induced apoptosis. *Exp. Cell. Res.*, **315**, 2420–2432.
14. Kato,T., Sato,N., Hayama,S., Yamabuki,T., Ito,T., Miyamoto,M., Kondo,S., Nakamura,Y. and Daigo,Y. (2007) Activation of Holliday junction recognizing protein involved in the chromosomal stability and immortality of cancer cells. *Cancer Res.*, **67**, 8544–8553.
15. Williams,R.S., Williams,J.S. and Tainer,J.A. (2007) Mre11-Rad50-Nbs1 is a keystone complex connecting DNA repair machinery, double-strand break signaling, and the chromatin template. *Biochem. Cell. Biol.*, **85**, 509–520.
16. Wang,Y., Broderick,P., Webb,E., Wu,X., Vijayakrishnan,J., Matakidou,A., Qureshi,M., Dong,Q., Gu,X., Chen,W.V. *et al.* (2008) Common 5p15.33 and 6p21.33 variants influence lung cancer risk. *Nat. Genet.*, **40**, 1407–1409.
17. Fabbro,M. and Henderson,B.R. (2003) Regulation of tumor suppressors by nuclear-cytoplasmic shuttling. *Exp. Cell. Res.*, **282**, 59–69.
18. Henderson,B.R. (2005) Regulation of BRCA1, BRCA2 and BARD1 intracellular trafficking. *Bioessays*, **27**, 884–893.
19. Ferrer,M., Rodriguez,J.A., Spierings,E.A., de Winter,J.P., Giaccone,G. and Kruyt,F.A. (2005) Identification of multiple nuclear export sequences in Fanconi anemia group A protein that contribute to CRM1-dependent nuclear export. *Hum. Mol. Genet.*, **14**, 1271–1281.
20. Neyton,S., Lespinasse,F., Lahaye,F., Staccini,P., Paquis-Flucklinger,V. and Santucci-Darmanin,S. (2007) CRM1-dependent nuclear export and dimerization with hMSH5 contribute to the regulation of hMSH4 subcellular localization. *Exp. Cell. Res.*, **313**, 3680–3693.
21. Fried,H. and Kutay,U. (2003) Nucleocytoplasmic transport: taking an inventory. *Cell. Mol. Life Sci.*, **60**, 1659–1688.
22. Friedrich,B., Quensel,C., Sommer,T., Hartmann,E. and Kohler,M. (2006) Nuclear localization signal and protein context both mediate importin alpha specificity of nuclear import substrates. *Mol. Cell. Biol.*, **26**, 8697–8709.
23. Kutay,U. and Guttinger,S. (2005) Leucine-rich nuclear-export signals: born to be weak. *Trends Cell. Biol.*, **15**, 121–124.
24. Henderson,B.R. and Eleftheriou,A. (2000) A comparison of the activity, sequence specificity, and CRM1-dependence of different nuclear export signals. *Exp. Cell. Res.*, **256**, 213–224.
25. Sorg,G. and Stamminger,T. (1999) Mapping of nuclear localization signals by simultaneous fusion to green fluorescent protein and to beta-galactosidase. *Biotechniques*, **26**, 858–862.
26. Plafker,S.M. and Macara,I.G. (2002) Ribosomal protein L12 uses a distinct nuclear import pathway mediated by importin 11. *Mol. Cell. Biol.*, **22**, 1266–1275.
27. van Hemert,M.J., Niemantsverdriet,M., Schmidt,T., Backendorf,C. and Spaink,H.P. (2004) Isoform-specific differences in rapid nucleocytoplasmic shuttling cause distinct subcellular distributions of 14-3-3 sigma and 14-3-3 zeta. *J. Cell. Sci.*, **117**, 1411–1420.
28. Luo,M., Pang,C.W., Gerken,A.E. and Brock,T.G. (2004) Multiple nuclear localization sequences allow modulation of 5-lipoxygenase nuclear import. *Traffic*, **5**, 847–854.
29. Tkach,J.M. and Glover,J.R. (2008) Nucleocytoplasmic trafficking of the molecular chaperone Hsp104 in unstressed and heat-shocked cells. *Traffic*, **9**, 39–56.
30. la Cour,T., Kiemer,L., Molgaard,A., Gupta,R., Skriver,K. and Brunak,S. (2004) Analysis and prediction of leucine-rich nuclear export signals. *Protein Eng. Des. Sel.*, **17**, 527–536.

31. la Cour,T., Gupta,R., Rapacki,K., Skriver,K., Poulsen,F.M. and Brunak,S. (2003) NESbase version 1.0: a database of nuclear export signals. *Nucleic Acids Res.*, **31**, 393–396.
32. Stauber,R., Gaitanaris,G.A. and Pavlakis,G.N. (1995) Analysis of trafficking of Rev and transdominant Rev proteins in living cells using green fluorescent protein fusions: transdominant Rev blocks the export of Rev from the nucleus to the cytoplasm. *Virology*, **213**, 439–449.
33. Kosugi,S., Hasebe,M., Matsumura,N., Takashima,H., Miyamoto-Sato,E., Tomita,M. and Yanagawa,H. (2009) Six classes of nuclear localization signals specific to different binding grooves of importin alpha. *J. Biol. Chem.*, **284**, 478–485.
34. Connor,M.K., Kotchetkov,R., Cariou,S., Resch,A., Lupetti,R., Beniston,R.G., Melchior,F., Hengst,L. and Slingerland,J.M. (2003) CRM1/Ran-mediated nuclear export of p27(Kip1) involves a nuclear export signal and links p27 export and proteolysis. *Mol. Biol. Cell.*, **14**, 201–213.
35. Ivanova,I.A. and Dagnino,L. (2007) Activation of p38- and CRM1-dependent nuclear export promotes E2F1 degradation during keratinocyte differentiation. *Oncogene*, **26**, 1147–1154.
36. Cheong,J.K., Gunaratnam,L. and Hsu,S.I. (2008) CRM1-mediated nuclear export is required for 26 S proteasome-dependent degradation of the TRIP-Br2 proto-oncoprotein. *J. Biol. Chem.*, **283**, 11661–11676.
37. Vandromme,M., Cavadore,J.C., Bonnieu,A., Froeschle,A., Lamb,N. and Fernandez,A. (1995) Two nuclear localization signals present in the basic-helix 1 domains of MyoD promote its active nuclear translocation and can function independently. *Proc. Natl Acad. Sci. USA*, **92**, 4646–4650.
38. Wen,S.T., Jackson,P.K. and Van Etten,R.A. (1996) The cytostatic function of c-Abl is controlled by multiple nuclear localization signals and requires the p53 and Rb tumor suppressor gene products. *EMBO J.*, **15**, 1583–1595.
39. Burich,R. and Lei,M. (2003) Two bipartite NLSs mediate constitutive nuclear localization of Mcm10. *Curr. Genet.*, **44**, 195–201.
40. Theodore,M., Kawai,Y., Yang,J., Kleshchenko,Y., Reddy,S.P., Villalta,F. and Arinze,I.J. (2008) Multiple nuclear localization signals function in the nuclear import of the transcription factor Nrf2. *J. Biol. Chem.*, **283**, 8984–8994.
41. Jones,S.M., Luo,M., Peters-Golden,M. and Brock,T.G. (2003) Identification of two novel nuclear import sequences on the 5-lipoxygenase protein. *J. Biol. Chem.*, **278**, 10257–10263.
42. Hu,W., Philips,A.S., Kwok,J.C., Eisbacher,M. and Chong,B.H. (2005) Identification of nuclear import and export signals within Fli-1: roles of the nuclear import signals in Fli-1-dependent activation of megakaryocyte-specific promoters. *Mol. Cell. Biol.*, **25**, 3087–3108.
43. Hanover,J.A., Love,D.C., DeAngelis,N., O'Kane,M.E., Lima-Miranda,R., Schulz,T., Yen,Y.M., Johnson,R.C. and Prinz,W.A. (2007) The High mobility group box transcription factor Nhp6Ap enters the nucleus by a calmodulin-dependent, Ran-independent pathway. *J. Biol. Chem.*, **282**, 33743–33751.
44. Keough,R.A., Macmillan,E.M., Lutwyche,J.K., Gardner,J.M., Tavner,F.J., Jans,D.A., Henderson,B.R. and Gonda,T.J. (2003) Myb-binding protein 1a is a nucleocytoplasmic shuttling protein that utilizes CRM1-dependent and independent nuclear export pathways. *Exp. Cell. Res.*, **289**, 108–123.
45. Yang,Y., Ma,J., Chen,Y. and Wu,M. (2004) Nucleocytoplasmic shuttling of receptor-interacting protein 3 (RIP3): identification of novel nuclear export and import signals in RIP3. *J. Biol. Chem.*, **279**, 38820–38829.
46. O'Brate,A. and Giannakakou,P. (2003) The importance of p53 location: nuclear or cytoplasmic zip code? *Drug. Resist. Updat.*, **6**, 313–322.
47. Rock,K.L., Gramm,C., Rothstein,L., Clark,K., Stein,R., Dick,L., Hwang,D. and Goldberg,A.L. (1994) Inhibitors of the proteasome block the degradation of most cell proteins and the generation of peptides presented on MHC class I molecules. *Cell*, **78**, 761–771.
48. Wojcik,C. and DeMartino,G.N. (2003) Intracellular localization of proteasomes. *Int. J. Biochem. Cell. Biol.*, **35**, 579–589.
49. Knauer,S.K., Carra,G. and Stauber,R.H. (2005) Nuclear export is evolutionarily conserved in CVC paired-like homeobox proteins and influences protein stability, transcriptional activation, and extracellular secretion. *Mol. Cell. Biol.*, **25**, 2573–2582.
50. von Mikecz,A. (2006) The nuclear ubiquitin-proteasome system. *J. Cell. Sci.*, **119**, 1977–1984.
51. Tembe,V. and Henderson,B.R. (2007) Protein trafficking in response to DNA damage. *Cell Signal*, **19**, 1113–1120.
52. Li,W., Yu,S., Liu,T., Kim,J.H., Blank,V., Li,H. and Kong,A.N. (2008) Heterodimerization with small Maf proteins enhances nuclear retention of Nrf2 via masking the NESzip motif. *Biochim. Biophys. Acta*, **1783**, 1847–1856.